

# INTERNATIONAL SOCIETY FOR SOIL MECHANICS AND GEOTECHNICAL ENGINEERING



*This paper was downloaded from the Online Library of the International Society for Soil Mechanics and Geotechnical Engineering (ISSMGE). The library is available here:*

<https://www.issmge.org/publications/online-library>

*This is an open-access database that archives thousands of papers published under the Auspices of the ISSMGE and maintained by the Innovation and Development Committee of ISSMGE.*

*The paper was published in the proceedings of the 1<sup>st</sup> International Conference on Scour of Foundations and was edited by Hamn-Ching Chen and Jean-Louis Briaud. The conference was held in Texas, USA, on November 17-20 2002.*

## **Local Scour Depths at Bridge Foundations: New Zealand Methodology**

By

Bruce Melville<sup>1</sup>

### **ABSTRACT**

A comprehensive method for estimating local scour depths at bridge foundations is presented. The method, which is presented in detail in Melville and Coleman (2000), was developed in New Zealand on the basis of an extensive series of laboratory investigations. Application of the method ensures that the various influences on local scour depths are systematically addressed. These are the characteristics of the flow approaching the bridge crossing, the shape of the river channel in the vicinity of the bridge, the characteristics of the bed sediments in the vicinity of the bridge, the geometry of the bridge foundations (piers and abutments), and the peak value and duration of the design flood. Application of the method is highlighted in two examples.

### **INTRODUCTION**

The major damage to bridges at river crossings occurs during floods. Damage is caused for various reasons, the main reason being riverbed scour at bridge foundations, namely piers and abutments. In New Zealand, at least one serious bridge failure each year (on average) can be attributed to scour of the bridge foundations. The damage can range from minor erosion at an adjacent river bank or bridge approach, to complete failure of the bridge structure or its road approach. Complete failure results in severe disruption to local traffic flows. The frequency of bridge failures due to scour has spurred many research projects of this vexing problem.

In spite of the significant investment in bridge scour research, bridges still fail due to scour. This has been a consequence of both inadequacies in design criteria adopted for older bridges and the lack of convenient and appropriate availability of the results of the past scour research to practitioners. A comprehensive treatment of the present state of knowledge on bridge scour is now available in Melville and Coleman (2000). The monograph, which makes use of New Zealand's extensive experience with scour problems, addresses all aspects of bridge scour, including general scour, contraction scour, local scour, scour countermeasures and 31 case histories of scour failures. The methodology for local scour is summarised in this paper. Examples of application of the local scour method are included.

### **ESTIMATION OF LOCAL SCOUR DEPTHS**

The method for estimation of local scour depths at bridge piers and abutments by Melville and Coleman (2000) is presented. The basic data required to apply the method are:

---

<sup>1</sup> Professor of Civil Engineering, The University of Auckland, Auckland, New Zealand

- **Approach flow**, characterised by the mean velocity ( $V$ ), depth ( $y$ ) and Manning's coefficient ( $n$ ) of the main channel. For bridge piers, the appropriate values of  $V$  and  $y$  are those, which best represent the flow approaching the particular pier.
- **Bed sediment**, characterised by the median size ( $d_{50}$ ), maximum size ( $d_{\max}$ ) and geometric standard deviation ( $\sigma_g$ ) of the particle size distribution. In practice,  $d_{90}$  (or a similar size) can be used in place of  $d_{\max}$ , which is unlikely to be known.
- **Foundation geometry**, characterised by the pier width ( $b$ ) and pier length ( $l$ ) for piers, abutment length ( $L$ ) for abutments, shape ( $Sh$ ) and alignment ( $\theta$ ). Circular piers are characterised by pier diameter ( $D$ ). For nonuniform piers, additional parameters are required, as described below.
- **Channel geometry (for abutments only)**, characterised by  $V$ ,  $y$ ,  $n$  and the depth ( $y^*$ ), Manning's coefficient ( $n^*$ ) and width ( $L^*$ ) of the flood channel.

The design method is based on the following relation for the depth of local scour:

$$d_s = K_{yB} K_I K_d K_s K_\theta K_G K_t \quad (1)$$

where the  $K$  factors are empirical expressions accounting for the various influences on scour depth:  $K_{yB}$  = depth-size  $\equiv K_{yb}$  for piers and  $K_{yL}$  for abutments;  $K_I$  = flow intensity;  $K_d$  = sediment size;  $K_s$  = pier or abutment shape;  $K_\theta$  = pier or abutment alignment;  $K_G$  = channel geometry ( $K_G \equiv 1$  for piers); and  $K_t$  = time.  $K_I$  is formulated to include sediment gradation effects as well as flow velocity effects.  $K_{yB} = f(y, B)$  and  $d_s$  have the dimension of length, while the other  $K$  factors are dimensionless.

The  $K$  factors are derived from envelope curves fitted to laboratory data. Expressions for the various  $K$  factors are summarised in Tables 1 and 2 and illustrated in Figures 1 and 2 for piers and abutments, respectively. For nonuniform piers, the pier width ( $b$ ) is replaced by the equivalent pier width ( $b_e$ ), as illustrated in Figure 3.

$K_I$  is a function of the threshold velocity ( $V_c$ ), the armour velocity ( $V_a$ ) and the velocity parameter  $[V - (V_a - V_c)]/V_c$ . The procedure for estimating these velocities is explained below and summarised in Tables 1 and 2.

### Maximum Possible Local Scour Depths at Piers and Abutments

The local scour depth is given by (1), in which  $K_I$ ,  $K_d$ ,  $K_G$  and  $K_t$  are always less than or equal to unity. Thus the maximum possible equilibrium local scour depth is

$$d_{se) \max} = K_{yB} K_s K_\theta \quad (2)$$

A simple equation for the maximum local scour depth at piers is obtained by substitution of the expression for  $K_{yB}$  for narrow piers in (2), giving

$$d_{se) \max} = 2.4 K_s K_\theta b \quad (3)$$

For design purposes, (3) is adequate for estimation of local scour depth at piers in many situations.

## PHYSICAL BASIS OF SCOUR DEPTH METHODOLOGY

The K-factors in (1) represent the various physical influences on local scour depth, as determined from systematic laboratory-based tests. In the following sections, each parameter is discussed briefly.

### Flow Depth - Foundation Size (Depth - Size) Factor, $K_{yB}$

Data, which demonstrate the influence of  $K_{yB} = f(y, B)$  on local scour depth, are given in Figure 4. The plot includes the reliable pier and abutment local scour depth data that are unaffected by flow intensity, sediment size, sediment gradation, foundation shape and alignment, channel geometry and time. The data plotted are from Chabert and Engeldinger (1956), Laursen and Toch (1956), Hancu (1971), Bonasoundas (1973), Basak (1975), Jain and Fischer (1979), Chee (1982), Chiew (1984), and Ettema (1980), for piers; and Gill (1972), Wong (1982), Tey (1984), Kwan (1984, 1988), Kandasamy (1989), and Dongol (1994), for abutments.

The solid lines in Figure 4 are envelopes to the data and apply, from left to right respectively, to wide (long), intermediate width (length) and narrow (short) piers (abutments) at threshold conditions. For clear-water scour at reduced flow velocities, lesser scour depths are developed. The equations of the upper-limit lines define the depth-size factors for piers, and are given in Tables 1 and 2.

### Flow Intensity Factor, $K_I$

$K_I$  represents the effects of flow intensity on local scour depth. It is defined, for each set of data, as the scour depth at a particular flow intensity divided by the maximum scour depth for the data set, where  $V$  is systematically varied for each data set and all other dependent parameters are held constant. The scour maxima used occur at the threshold peak for uniform sediments and the live-bed peak for nonuniform sediments.

Figure 5 (uniform sediments) and Figure 6 (nonuniform sediments) are plots of laboratory data from many sources for local scour at piers and abutments in terms of  $K_I$ . The nonuniform sediment data are plotted in terms of a transformed velocity parameter, as shown. The transformed velocity parameter aligns the armour peaks (that is  $V=V_a$ ) for nonuniform sediments with varying  $\sigma_g$  with the threshold peak (that is  $V=V_c$ ) for uniform sediments. For uniform sediments,  $V_a \equiv V_c$  and  $[V-(V_a-V_c)]/V_c \equiv V/V_c$ . The transformed velocity parameter incorporating  $V_a$  largely accounts for the effects of sediment nonuniformity as well as those of flow velocity, although the smaller values of scour depth at  $[V-(V_a-V_c)]/V_c \approx 1$ , as  $\sigma_g$  increases, remain. Thus, the effects of sediment nonuniformity are mostly accounted for in the flow intensity factor. It is apparent that all of the data are enveloped by a value of  $K_I$  increasing linearly from zero to unity at the threshold condition and thereafter remaining unchanged.

The velocities  $V_c$  and  $V_a$  can be determined using the logarithmic velocity distribution equation:

$$\frac{V_c}{u_{*c}} = 5.75 \log \left( 5.53 \frac{y}{d_{50}} \right) \quad (4)$$

where  $u_{*c}$  is critical shear velocity determined from the Shields' diagram, and  $d_{50}$  and  $u_{*c}$  are replaced by  $d_{50a}$  (median size of the armour layer =  $d_{\max}/1.8$ ) and  $u_{*ca}$  (critical shear velocity of the armour layer), respectively, for determination of the armour peak velocity,  $V_a$ .

Figure 7 is a comparison of U.S. field data with the laboratory-based envelope curves for  $K_I$ . Because many of these data were collected at sites where the bed material is nonuniform, the transformed velocity parameter is used in Figure 7. The field scour depths are normalised using the projected pier width,  $b_p$ , to compensate for pier skewness effects inherent in the data. The armour peak velocity was determined assuming  $d_{84}$  to be representative of the maximum grain size in the bed material. The laboratory-derived  $K_I$  function also envelopes the field data.

#### **Sediment Size Factor, $K_d$**

The pier data by Ettema (1980), Chiew (1984) and Baker (1986) and the abutment data by Dongol (1994) are plotted in Figure 8 in terms of the sediment size multiplying factor,  $K_d$ , which is defined generally as the ratio of the scour depth for a particular  $B/d_{50}$  to that for  $B/d_{50} \geq 50$ . The data for uniform and nonuniform sediments are plotted separately. The plots show that the influence of relative sediment size on scour depth is the same for both piers and abutments, although few data are shown for abutments. Because the condition  $L/d_{50} < 50$  is unlikely in practice, it is considered that the few abutment data shown in Figure 8 are adequate for definition of  $K_d$  for abutments.

Nonuniform sediments are characterised by channel bed armouring as discussed earlier. The nonuniform sediment data in Figure 8 are plotted for different values of the velocity parameter  $[V - (V_a - V_c)]/V_c = 1.0, 2.0, 3.0$  and  $4.0$ . The data are plotted in terms of  $b/d_{50a}$  or  $L/d_{50a}$  because the median size of the armour layer is considered to be the characteristic sediment size. The envelope curves in Figure 8 define the sediment size factor for design purposes.

#### **Foundation Shape Factor, $K_s$**

The shape factor  $K_s$  is defined as the ratio of the scour depth for a particular foundation shape to that for the standard shapes, namely circular piers and vertical-wall abutments.

Recommended shape factors for uniform piers, i.e. piers having constant cross-sectional shape, are given in Table 1. These factors, taken from Melville (1997), show that shape is relatively insignificant for uniform piers. The shape factors should only be used where the pier is aligned with the flow, that is,  $K_s = 1$  for a skewed pier.

The four cases of local scour at nonuniform piers, where the pier is founded on a wider element (caissons, slab footings and pile caps), are shown in Figure 3. For **Case I**, the local scour is estimated using the pier width  $b$ . For **Case II**, a procedure given by Melville and Raudkivi (1996) to estimate the size of an equivalent uniform pier can be applied. The equivalent uniform pier induces (at least) the same scour as the nonuniform pier. The procedure is therefore conservative. Melville and Raudkivi (1996), who measured scour depths at a circular pier founded on a larger concentric, circular caisson, give the following relation:

$$b_e = b \left( \frac{y + Y}{y + b^*} \right) + b^* \left( \frac{b^* - Y}{b^* + y} \right) \quad (5)$$

where  $b_e$  = width of an equivalent uniform pier;  $b^*$  = caisson width; and the equation is restricted to the range defined by  $Y \leq b^*$  and  $-Y \leq y$ , where  $Y$  represents the elevation of the top surface of the caisson (Figure 3). The relation for  $b_e$  can be used for Case II nonuniform piers that are geometrically similar to the caisson foundation shown in Figure 3, including piers founded on slab footings and piled foundations, unless the footing or the pile cap is

undermined by the scour. Equation 5 also applies to **Case III** caisson foundations and may be used to give conservative scour estimates for Case III piled foundations. For **Case IV** caisson foundations, the local scour is estimated using the caisson width  $b^*$ . This approach would also give a conservative estimate of Case IV local scour at a piled foundation.

Also given in Figure 3 and Table 1 is a method to determine the effective size of a bridge pier having a raft of floating debris material attached.

Shape factors, based on data by Hannah (1978), for piled pier foundations where the pile cap is clear of the water surface (Case V) are given in Table 1 and illustrated in Figure 3 (Case V). The pile-group shape factor values are shown in Table 1 for a single row and a double row of piles in terms of approach flow angle,  $\theta$ , pile diameter,  $D_p$  and pile spacing (measured centre-to-centre),  $S_p$ . The single-row values apply also to a pier comprising a row of cylinders. The values shown include pier alignment effects and shape effects, that is, they represent  $K_s K_\theta$ .

Recommended shape factors for shorter abutments are given in Table 2. For longer abutments, shape effects are less significant, and an adjusted shape factor  $K_s^*$  is applied.  $K_s^*$  is given in Table 2.

#### **Foundation Alignment Factor, $K_\theta$**

The alignment factor  $K_\theta$  is defined as the ratio of the local scour depth at a skewed bridge foundation to that at an aligned foundation. Bridge piers are aligned if  $\theta = 0^\circ$ , while abutments are considered to be aligned where  $\theta = 90^\circ$ . An equation for  $K_\theta$  for non-cylindrical piers is given in Table 1.

Recommended alignment factors for longer abutments are given in Table 2. For shorter abutments, alignment effects are less significant. The adjusted alignment factor  $K_\theta^*$  for shorter abutments is given in Table 2.

#### **Approach Channel Geometry Factor, $K_G$**

The approach channel geometry factor  $K_G$  is the ratio of the local scour depth at a bridge foundation to that at the same foundation sited in the equivalent rectangular channel. The local scour at bridge piers is considered to be unaffected by approach channel geometry as long as appropriate values of  $y$  and  $V$  are used to estimate the scour depth. If values of  $y$  and  $V$  are selected to be representative of the flow approaching the particular pier,  $K_G=1.0$ .

For bridge abutments in rectangular channels (Case A of Figure 2),  $K_G=1.0$  by definition. For abutments in compound channels,  $K_G$  depends on the position of the abutment in the compound channel (Figure 2). At Case B abutments, the equation given in Table 2 is recommended, where  $L$  and  $L^*$  = total projected length of the abutment (including the bridge approach) and projected length of the abutment (including the bridge approach) spanning the flood channel, respectively;  $y$  and  $y^*$  = flow depths in the main and flood channels, respectively; and  $n$  and  $n^*$  = Manning roughness coefficients for the main and flood channels, respectively. The equation is derived from a simple theoretical analysis based on the ratio of flows deflected by the abutment, including the bridge approach, in a compound channel to such flows in the corresponding rectangular channel. The equation is plotted in Figure 9 for ranges of values of the ratios  $(L^*/L)$ ,  $(y/y^*)$  and  $(n/n^*)$ . Case C can be considered to be a special condition of Case A if the flow in the main channel is ignored; thus  $K_G=1.0$ . For Case D abutments where the abutment is sited at about the edge of the main channel,  $K_G$  can be estimated from the equation for Case B, with  $L^*/L=1.0$ . No specific information is available to aid estimation of  $K_G$  for other Case D abutments; such situations could be treated by

interpolating conservatively between scour depth estimates for longer (Case B) and shorter (Case C) abutments sited in the same channel.

#### **Time Factor, $K_t$**

The time factor is defined as the ratio of local scour depth  $d_s$  at a particular time  $t$  to the equilibrium scour depth  $d_{se}$ , which occurs at time  $t_e$ . The value of  $K_t$  at a site depends on whether conditions are clear-water or live-bed. Under live-bed conditions, the equilibrium depth of local scour is attained rapidly and  $K_t = 1.0$  can be assumed.

Functions for the time factor at piers and abutments are given in Tables 1 and 2, respectively. The latter is derived from recent research and represents an updating of the recommendations in Melville and Coleman (2000).  $K_t$  depends on  $t_e$ , the time to equilibrium scour depth. Equations for estimation of  $t_e$  are also given in Tables 1 and 2.

### **EXAMPLES OF APPLICATION OF METHODOLOGY**

#### **Local scour at piers**

A bridge pier, comprising a piled foundation, is situated in the 310 m wide flood channel of a river crossing, as illustrated in Figure 10. The peak flow rate in the flood channel is  $500 \text{ m}^3/\text{s}$  and this persists for 1 day. The calculations are presented in Table 3, showing a local scour depth of 1.71 m.

#### **Local scour at abutments (including contraction scour)**

A bridge is situated at a channel bend, as illustrated in Figure 11. The sediment is a medium sand with  $d_{50} = 0.5 \text{ mm}$ . The peak flow rate is  $440 \text{ m}^3/\text{s}$  and this lasts for 2 days. The calculations are presented in Table 4, showing local scour depth of 3.83 m.

Contraction scour would occur due to the bridge narrowing the channel. Mobile-bed conditions would exist (Table 4). Laursen's (1960) equation for contraction scour is used to estimate the contraction scour depth. The equation is

$$\frac{y_2}{y_1} = \left( \frac{Q_2}{Q_{1m}} \right)^{6/7} \left( \frac{W_1}{W_2} \right)^{k_1} \quad (5)$$

where  $y_1$  = average depth in the approach main channel;  $y_2$  = average depth in the main channel of the contracted section;  $W_1$  = bottom width of the approach main channel;  $W_2$  = bottom width of the main channel in the contracted section;  $Q_{1m}$  = discharge in the approach main channel transporting sediment;  $Q_2$  = total discharge through the bridge; and  $k_1$  = a coefficient depending on the mode of sediment transport. For the given example  $Q_{1m} = Q_2$ .

## REFERENCES

- Basak, V. (1975) "Scour at square piles," Report No. 583, Devlet Su isleri genel mudurlugu, Ankara, Turkey.
- Bonasoundas, M. (1973) "Strömungsvorgang und kolkproblem," Report No. 28, Oskar v. Miller Institut, Tech. Univ. Munich, Germany.
- Baker, R.E. (1986) "Local scour at bridge piers in non-uniform sediment," Report No. 402, School of Engineering, The University of Auckland, Auckland, New Zealand, 91pp.
- Chabert, J. and Engeldinger, P. (1956) "Etude des affouillements autour des piles des ponts," Laboratoire d'Hydraulique, Chatou, France (in French).
- Chee, R.K.W. (1982) "Live-bed scour at bridge piers," Report No. 290, School of Engineering, The University of Auckland, Auckland, New Zealand, 79pp.
- Chiew, Y.M. (1984) "Local scour at bridge piers," Report No. 355, School of Engineering, The University of Auckland, Auckland, New Zealand, 200pp.
- Dongol, D. M. S. (1994). "Local scour at bridge abutments." Report No. 544, School of Engineering, The University of Auckland, Auckland, New Zealand, 409pp.
- Ettema, R. (1980) "Scour at bridge piers," Report No. 216, School of Engineering, The University of Auckland, Auckland, New Zealand, 527pp.
- Gill, M.A. (1972) "Erosion of sand beds around spur dikes," Journal of the Hydraulics Division, A.S.C.E., 98(9), 1587-1602.
- Hancu, S. (1971) "Sur le calcul des affouillements locaux dans la zone des piles des ponts," Proc., 14<sup>th</sup>. I.A.H.R. Congress, Paris, France, Vol. 3, 299-313.
- Hannah, C.R. (1978) "Scour at pile groups," Report No. 78-3, Department of Civil Engineering, University of Canterbury, Christchurch, New Zealand, 92pp.
- Jain, S.C. and Fischer, E.E. (1979) "Scour around bridge piers at high Froude numbers," Report No. FH-WA-RD-79-104, Federal Highway Administration, U.S. Department of Transportation, Washington, D.C., U.S.A.
- Kandasamy, J.K. (1989) "Abutment scour," Report No. 458, School of Engineering, The University of Auckland, Auckland, New Zealand, 278pp.
- Kwan, T. F. (1984). "Study of abutment scour." Report No. 328, School of Engineering, The University of Auckland, Auckland, New Zealand, 225pp.
- Kwan, T.F. (1988) "A study of abutment scour," Report No. 451, School of Engineering, The University of Auckland, Auckland, New Zealand, 461pp.
- Laursen, E.M. (1960) "Scour at bridge crossings," Journal of the Hydraulics Division, A.S.C.E., 86(2), 39-54.
- Laursen, E.M. and Toch, A. (1956) "Scour around bridge piers and abutments," Bulletin No.4, Iowa Highways Research Board, Ames, Iowa, U.S.A.



Melville, B. W. (1997). "Pier and abutment scour - an integrated approach." J. Hyd. Engrg., ASCE, 123(2), 125-136.

Melville, B. W., and Chiew, Y. M. (1999). "Time scale for local scour at bridge piers." J. Hyd. Engrg., ASCE, 125(1), 59-65.

Melville, B. W., and Coleman, S. E. (2000). Bridge scour. Water Resources Publications, LLC, Colorado, U.S.A. 550pp.

Melville, B.W. and Raudkivi, A.J. (1996) "Effects of foundation geometry on bridge pier scour," Journal of Hydraulic Engineering, A.S.C.E., 122(4), 203-209.

Neill, C.R. (1987) "Bridge hydraulics - An update report," Roads and Transportation Assoc. of Canada, Ottawa, Canada, 75pp.

Tey, C. B. (1984). "Local scour at bridge abutments." Report No. 329, School of Engineering, The University of Auckland, Auckland, New Zealand, 111pp.

Wong, W.H. (1982) "Scour at bridge abutments," Report No. 275, School of Engineering, The University of Auckland, Auckland, New Zealand, 109pp.

**Table 1 Factors influencing local scour depth at bridge piers**

Factor	K	Method of Estimation				
Depth-size factor	K <sub>y<sub>b</sub></sub>	$K_{yb} = 2.4b$		$\frac{b}{y} < 0.7$		
		$K_{yb} = 2\sqrt{yb}$		$0.7 < \frac{b}{y} < 5$		
		$K_{yb} = 4.5y$		$\frac{b}{y} > 5$		
Flow intensity factor	K <sub>I</sub>	For uniform sediments: d <sub>50a</sub> ≡ d <sub>50</sub> and V <sub>a</sub> ≡ V <sub>c</sub> For nonuniform sediments: d <sub>50a</sub> = d <sub>max</sub> /1.8 ≈ d <sub>84</sub> /1.8 = σ <sub>g</sub> d <sub>50</sub> /1.8; and V <sub>a</sub> = 0.8V <sub>ca</sub> , where V <sub>ca</sub> is V <sub>c</sub> calculated for d <sub>50a</sub>				
		$K_I = \frac{V - (V_a - V_c)}{V_c}$		$\frac{V - (V_a - V_c)}{V_c} < 1$		
		$K_I = 1$		$\frac{V - (V_a - V_c)}{V_c} \geq 1$		
Sediment size factor	K <sub>d</sub>	$K_d = 0.57 \log \left( 2.24 \frac{b}{d_{50}} \right)$		$\frac{b}{d_{50}} \leq 25$		
		$K_d = 1.0$		$\frac{b}{d_{50}} > 25$		
Shape factor	K <sub>s</sub>	Shape			K <sub>s</sub>	
		Circular			1.0	
		Round Nosed			1.0	
		Square Nosed			1.1	
		Sharp Nosed			0.9	
		Skewed piers			1.0	
Equivalent size for nonuniform piers	b <sub>e</sub>	$b_e = b$			Case I	
		$b_e = b \left( \frac{y + Y}{y + b^*} \right) + b^* \left( \frac{b^* - Y}{b^* + y} \right) \quad Y \leq b^*, -Y \leq y$			Case II Case III	
		$b_e = b^*$			Case IV	
Multiplying factors for pile groups	K <sub>s</sub> K <sub>θ</sub>	Type	S <sub>p</sub> /D <sub>p</sub>	K <sub>s</sub> K <sub>θ</sub>		
				θ<5°	θ=5°→45°	θ=90°
		Single Row	2	1.12	1.40	1.20
			4	1.12	1.20	1.10
			6	1.07	1.16	1.08
			8	1.04	1.12	1.02
			10	1.00	1.00	1.00
		Double Row	2	1.50	1.80	-
			4	1.35	1.50	-
Alignment factor	K <sub>θ</sub>	$K_\theta = \left( \frac{l}{b} \sin \theta + \cos \theta \right)^{0.65}$ non - circular piers				
		$K_\theta = 1.0$ circular piers				

Time factor	$K_t$	$K_t = \exp \left\{ -0.03 \left  \frac{V_c}{V} \ln \left( \frac{t}{t_e} \right) \right ^{1.6} \right\} \quad \frac{V}{V_c} \leq 1$ $K_t = 1.0 \quad \frac{V}{V_c} > 1$
Equilibrium time	$t_e$	$t_e (days) = 48.26 \frac{b}{V} \left( \frac{V}{V_c} - 0.4 \right) \quad \frac{y}{b} > 6, \frac{V}{V_c} > 0.4$ $t_e (days) = 30.89 \frac{b}{V} \left( \frac{V}{V_c} - 0.4 \right) \left( \frac{y}{b} \right)^{0.25} \quad \frac{y}{b} \leq 6, \frac{V}{V_c} > 0.4$
Equivalent size - pier with debris	$b_e$	$b_e = \frac{0.52 T_d b_d + (y - 0.52 T_d) b}{y}$

**Table 2 Factors influencing local scour depth at bridge abutments**

Factor	K	Method of Estimation	
Flow depth-abutment size	$K_{yL}$	$K_{yL} = 10y \quad \frac{y}{L} \leq 0.04$ $K_{yL} = 2\sqrt{yL} \quad 0.04 < \frac{y}{L} \leq 1$ $K_{yL} = 2L \quad \frac{y}{L} > 1$	
Flow intensity	$K_I$	<p>For uniform sediments: <math>d_{50a} \equiv d_{50}</math> and <math>V_a \equiv V_c</math>  For nonuniform sediments:  <math>d_{50a} = d_{max}/1.8 \approx d_{84}/1.8 = \sigma_g d_{50}/1.8</math>; and  <math>V_a = 0.8 V_{ca}</math>, where <math>V_{ca}</math> is <math>V_c</math> calculated for <math>d_{50a}</math></p> $K_I = \frac{V - (V_a - V_c)}{V_c} \quad \text{for } [V - (V_a - V_c)]/V_c < 1$ $K_I = 1.0 \quad \text{for } [V - (V_a - V_c)]/V_c \geq 1$	
Sediment size	$K_d$	$K_d = 1.0 \quad \frac{L}{d_{50a}} > 60$	
Foundation shape		Shape	$K_s$
	$K_s$	Vertical-wall Wing-wall Spill-through 0.5:1 (H:V) Spill-through 1:1 Spill-through 1.5:1	1.0 0.75 0.6 0.5 0.45
	$K_s^*$	$K_s^* = K_s \quad \frac{L}{y} \leq 10$ $K_s^* = K_s + 0.667(1 - K_s) \left( 0.1 \frac{L}{y} - 1 \right) \quad 10 < \frac{L}{y} < 25$ $K_s^* = 1.0 \quad \frac{L}{y} \geq 25$	

Foundation alignment	$K_\theta$	$\theta$ (°)	30	45	60	90	120	135	150
		$K_\theta$	0.90	0.95	0.98	1.0	1.05	1.07	1.08
	$K_\theta^*$	$K_\theta^* = 1.0$ $\frac{L}{y} \leq 1$							
		$K_\theta^* = K_\theta + (1 - K_\theta) \left( 1.5 - 0.5 \frac{L}{y} \right)$ $1 < \frac{L}{y} < 3$							
		$K_\theta^* = 1.0$ $\frac{L}{y} \leq 1$							
Approach-channel geometry		Case A (Fig. 2): [Simple rectangular river channel] $K_G \equiv 1.0$							
		Case C (Fig. 2): [Abutment well back from the flood-channel edge] Consider only the flood channel flows of $y^*$ and set $K_G = 1.0$							
	$K_G$	Case B (Fig. 2): [Abutment in the main channel] $K_G = \sqrt{1 - \left( \frac{L^*}{L} \right) \left[ 1 - \left( \frac{y^*}{y} \right)^{5/3} \left( \frac{n}{n^*} \right) \right]}$							
		Case D (Fig. 2): [Abutment near the flood channel edge] Abutment at about the flood-channel edge: Case B with $L^*/L=1.0$ .							
Time		$t_e(days) = 20.83 \frac{L}{V} \left( \frac{V}{V_c} \right)^3 \left( \frac{y}{L} \right)^{0.8}$ for $y/L < 1$							
		$t_e(days) = 20.83 \frac{L}{V} \left( \frac{V}{V_c} \right)^3$ for $y/L \geq 1$							
	$K_t$	$K_t = \exp \left[ -0.07 \left( \frac{V}{V_c} \right)^{-1} \left  \ln \left( \frac{t}{t_e} \right) \right ^{1.5} \right]$ for $V/V_c < 1$ $K_t = 1.0$ for $V/V_c \geq 1$							

**Table 3 Pier Scour Example**

$b_e = b \left( \frac{y_f + Y}{y_f + b^*} \right) + b^* \left( \frac{b^* - Y}{b^* + y_f} \right) = 0.6 \left( \frac{2.0 - 0.6}{2.0 + 1.5} \right) + 1.5 \left( \frac{1.5 + 0.6}{1.5 + 2.0} \right) = 1.14 \text{ m}$
$\frac{b_e}{y} = 0.57, K_{yb} = 2.4b_e = 2.74 \text{ m}$
$K_s = 1.0$ , for skewed pier
$K_\theta = \left( \frac{l}{b_e} \sin \theta + \cos \theta \right)^{0.65} = 1.93$
$V = \frac{Q_f}{W_{1f} y_f} = \frac{500}{310 \times 2} = 0.81 \text{ m/s}$

From grading curve, $d_{\max} = 27 \text{ mm}$ $d_{50a} = \frac{d_{\max}}{1.8} = 15 \text{ mm}, u_{*c} = 0.067 \text{ m/s}, u_{*ca} = 0.118 \text{ m/s}$ $V_c = 1.29 \text{ m/s}, V_{ca} = 1.95 \text{ m/s}, V_a = 1.56 \text{ m/s}, \frac{V - (V_a - V_c)}{V_c} = 0.42, K_I = 0.42$
$\frac{y}{b_e} = 1.75, t_e (\text{days}) = 30.89 \frac{b_e}{V} \left( \frac{V}{V_c} - 0.4 \right) \left( \frac{y}{b_e} \right)^{0.25} = 11.4 \text{ days}$
$K_t = \exp \left\{ -0.03 \left  \frac{V_c}{V} \ln \left( \frac{t}{t_e} \right) \right ^{1.6} \right\} = 0.77$
$\frac{b_e}{d_{50}} = 228, \frac{b_e}{d_{50a}} = 76, K_d = 1.0$
$d_s = K_{yb} K_I K_d K_s K_\theta K_t = 1.71 \text{ m}$

**Table 4 Abutment Scour Example**

The threshold velocity is, $V_c = 1.3 \text{ m/s}$ , for $y = 6 \text{ m}$ and $d_{50} = 0.5 \text{ mm}$ (using Neill's 1987 competent velocity chart. $V_2 = \frac{Q}{W_2 y} = \frac{440}{19 \times 6} = 3.86 \text{ m/s} \gg V_c$ and conditions are live-bed
Using (5) with $k_1 = 0.69$ to estimate contraction scour: $\frac{d_s}{y_1} = \left( \frac{W_1}{W_2} \right)^{k_1} - 1, d_{s \text{ contraction}} = 1.25 \text{ m}$ $d_{s \text{ contraction}} = 1.5 \text{ m, RHS}, d_{s \text{ contraction}} = 1.0 \text{ m, LHS}$ It is assumed that the contraction scour is distributed as shown in Figure 11
Flow depth after contraction scour is: $y = 6 + d_{s \text{ contraction}} = 7.25 \text{ m}$
$\frac{L}{y} = 0.42, K_{yL} = 6 \text{ m}$
$V = \frac{Q}{W_1 y} = \frac{440}{25 \times 7.25} = 2.43 \text{ m/s}$
$u_{*c} = 0.016 \text{ m/s}, V_c = 0.45 \text{ m/s}, \frac{V}{V_c} = 5.4, K_I = 1.0$ and $K_t = 1.0$ for live - bed conditions
$\frac{L}{d_{50}} > 25, K_d = 1.0$
$K_s = 0.75$ , for wing - wall abutment, $K_s^* = K_s$
$\frac{L}{y} < 1, K_{\theta \text{ LHS}} = K_{\theta \text{ RHS}} = 1.0$
$K_G = 1.0$
$d_s = K_{yL} K_I K_d K_s K_\theta K_G K_t, d_s = 4.5 \text{ m}$

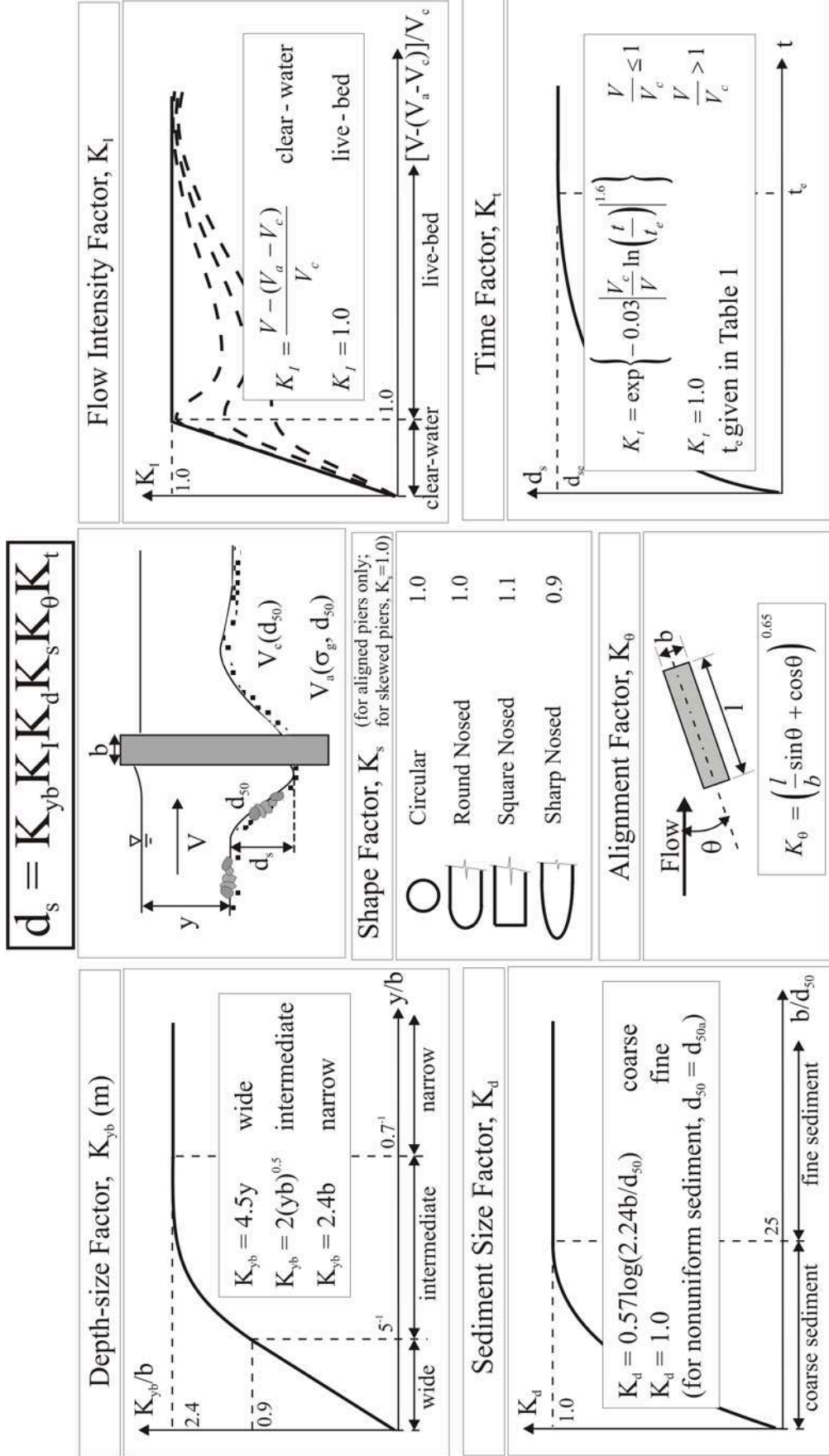


**Figure 1 Method for estimation of local scour depth at piers.**

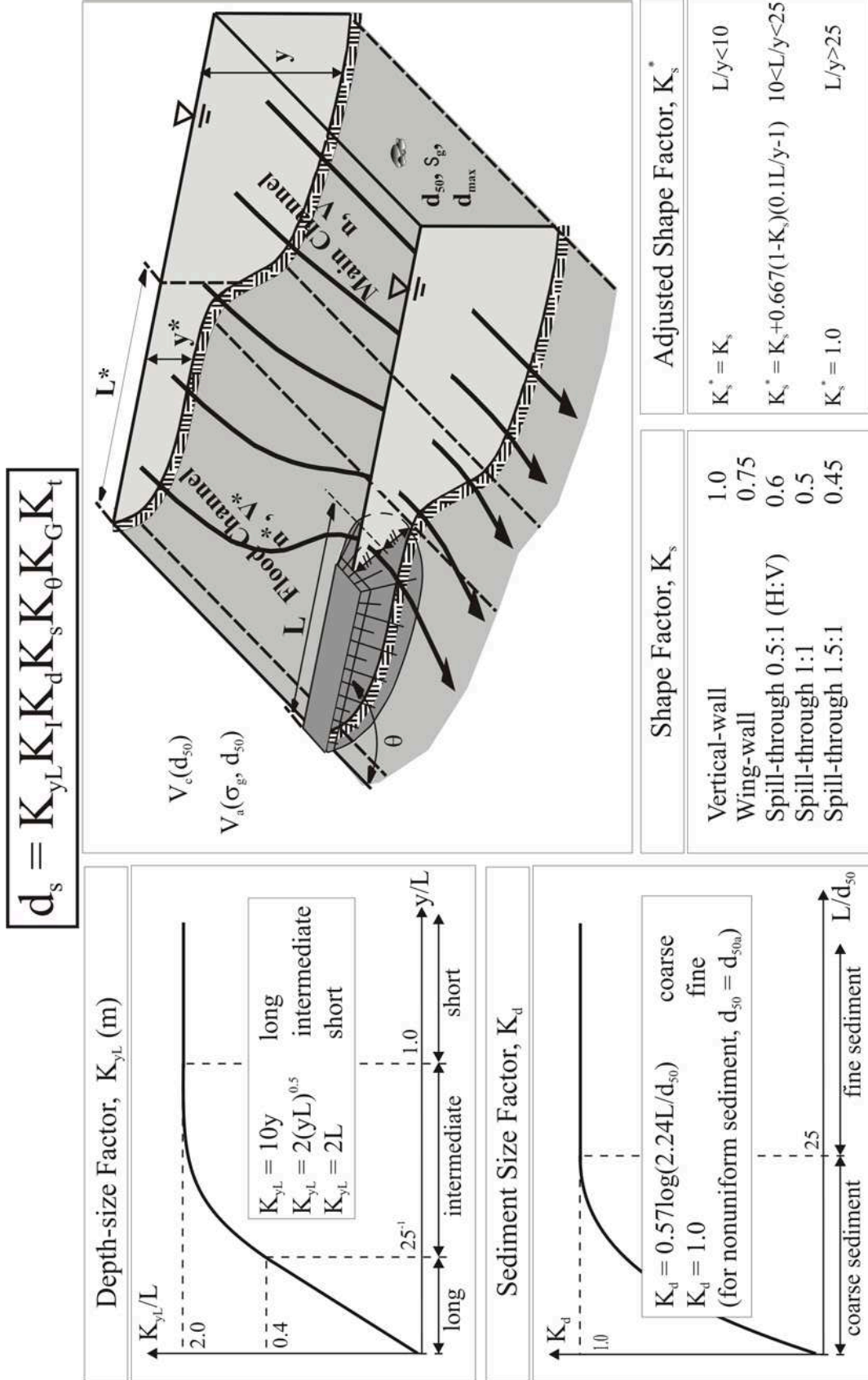


Figure 2 Method for estimation of local scour depth at abutments.

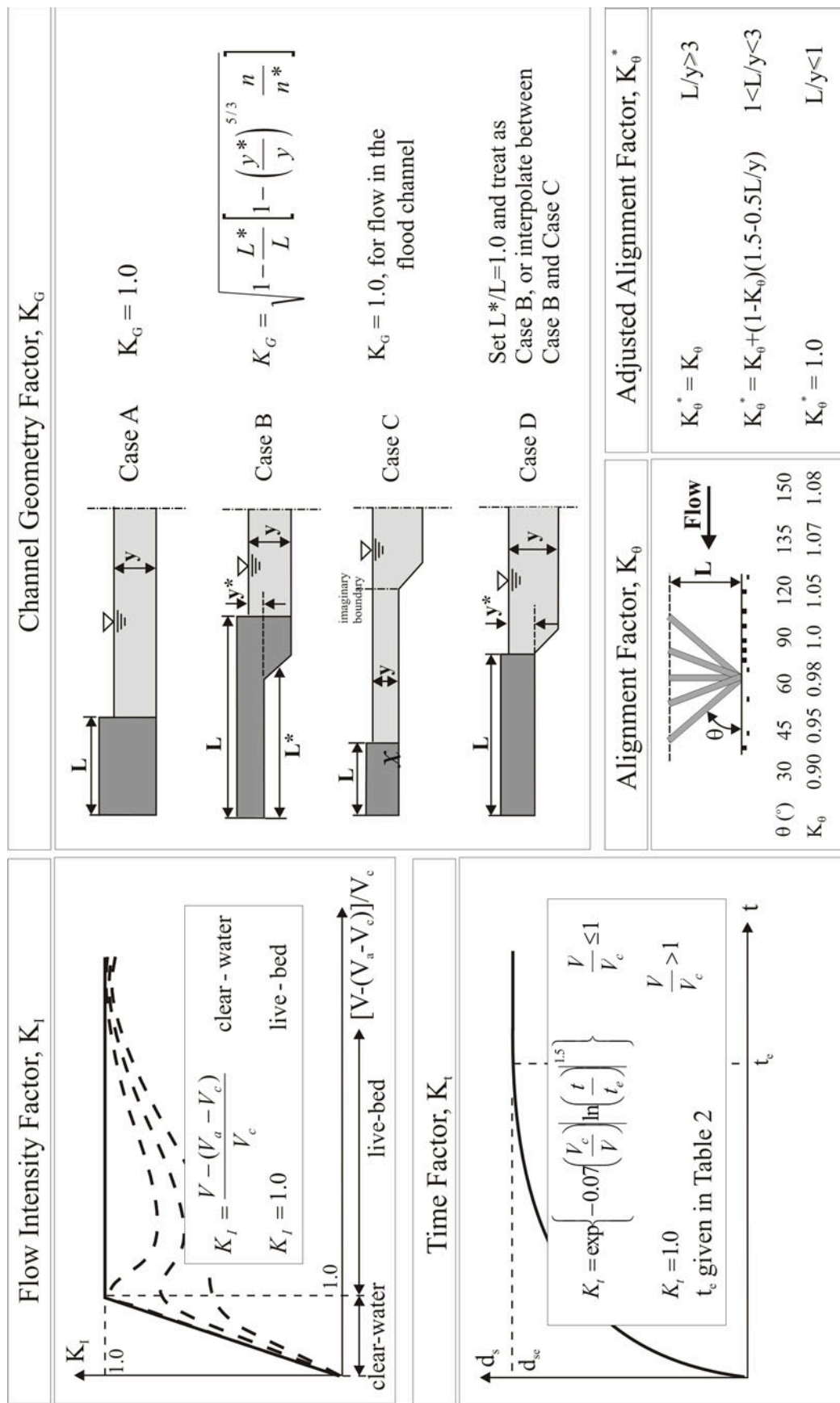


Figure 2 (cont.) Method for estimation of local scour depth at abutments.



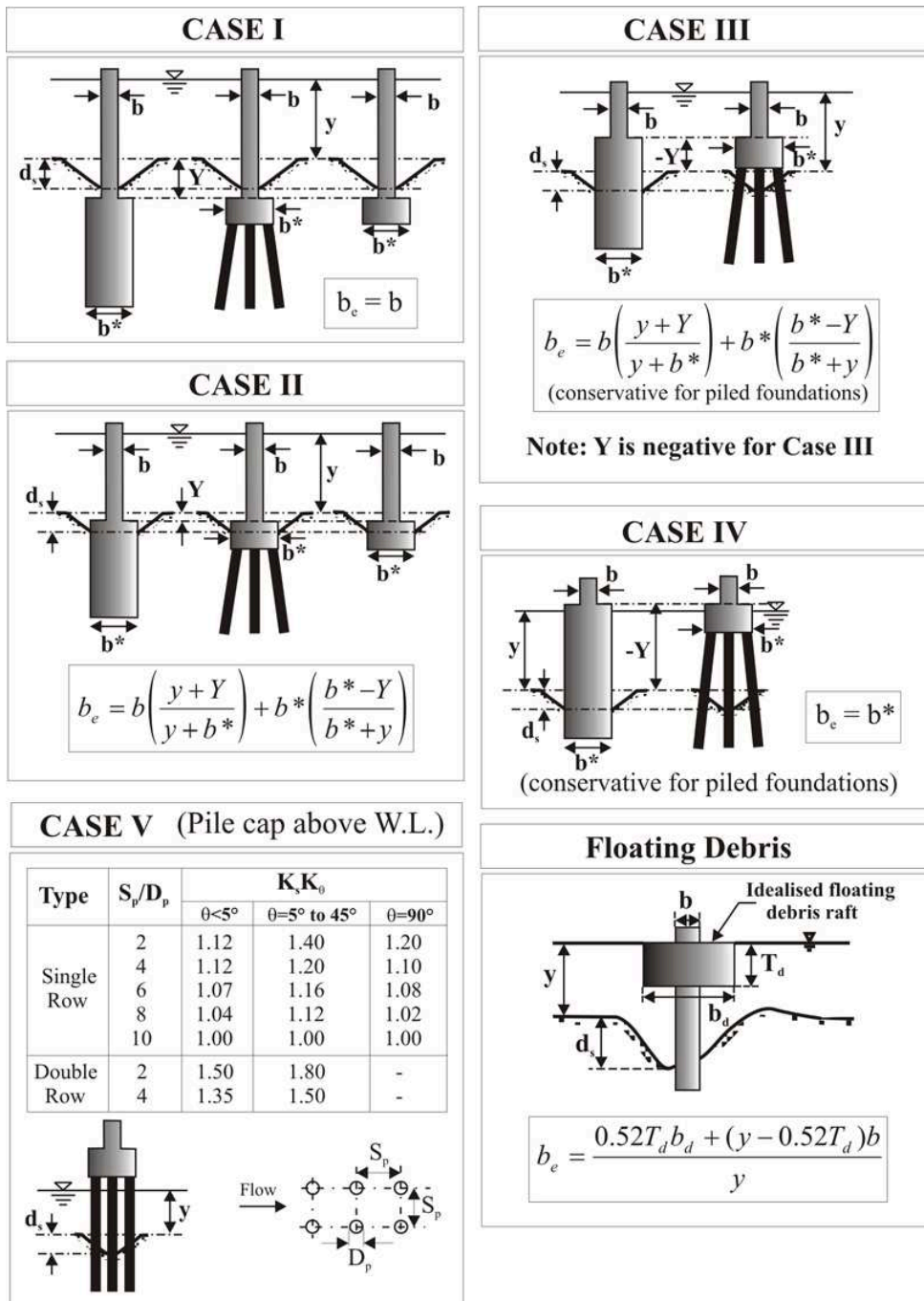


Figure 3 Method for estimation of local scour depth at nonuniform piers

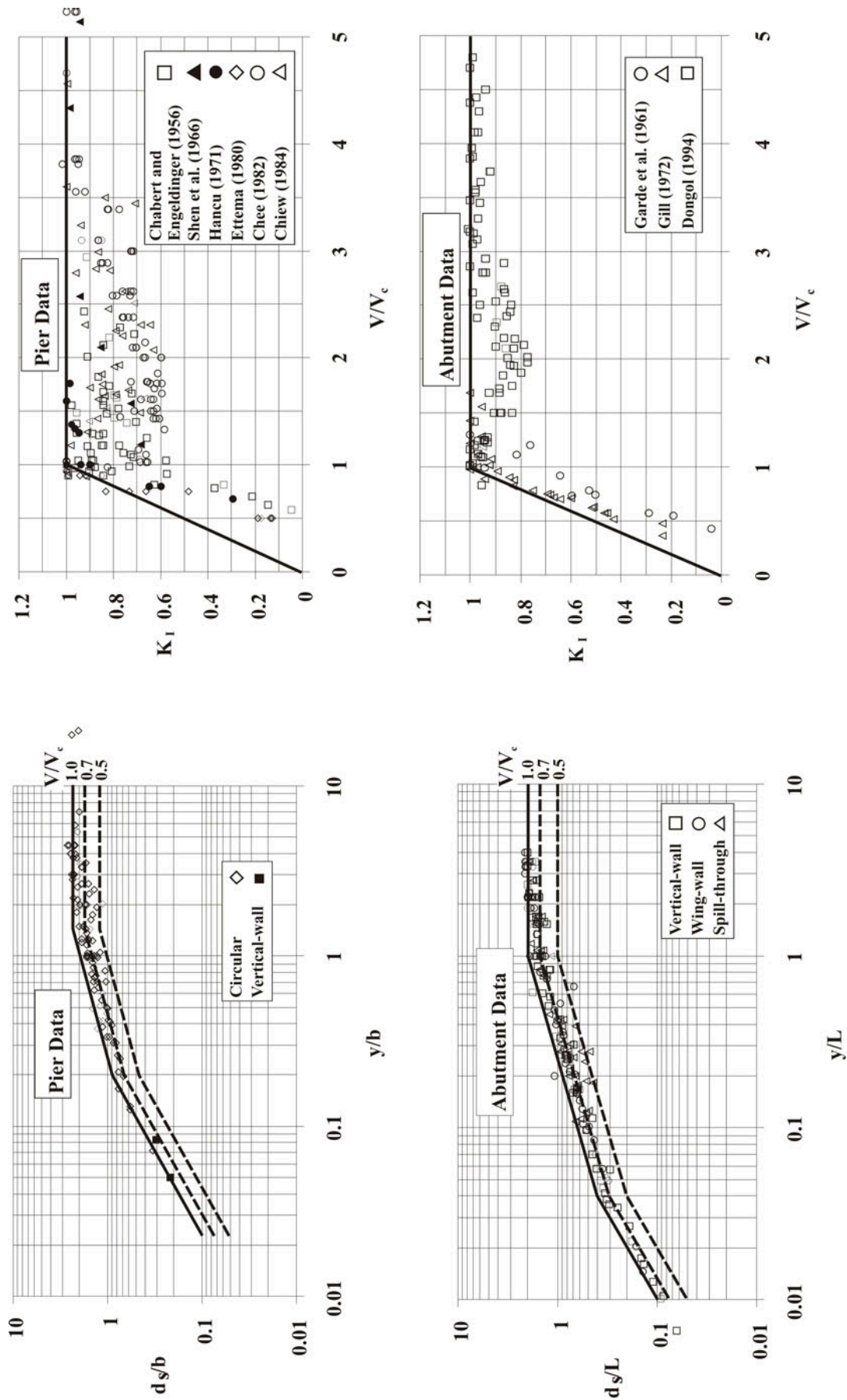


Figure 5 The influence of flow intensity on local scour depth in uniform sediment

Figure 4 The influence of flow shallowness on local scour depth

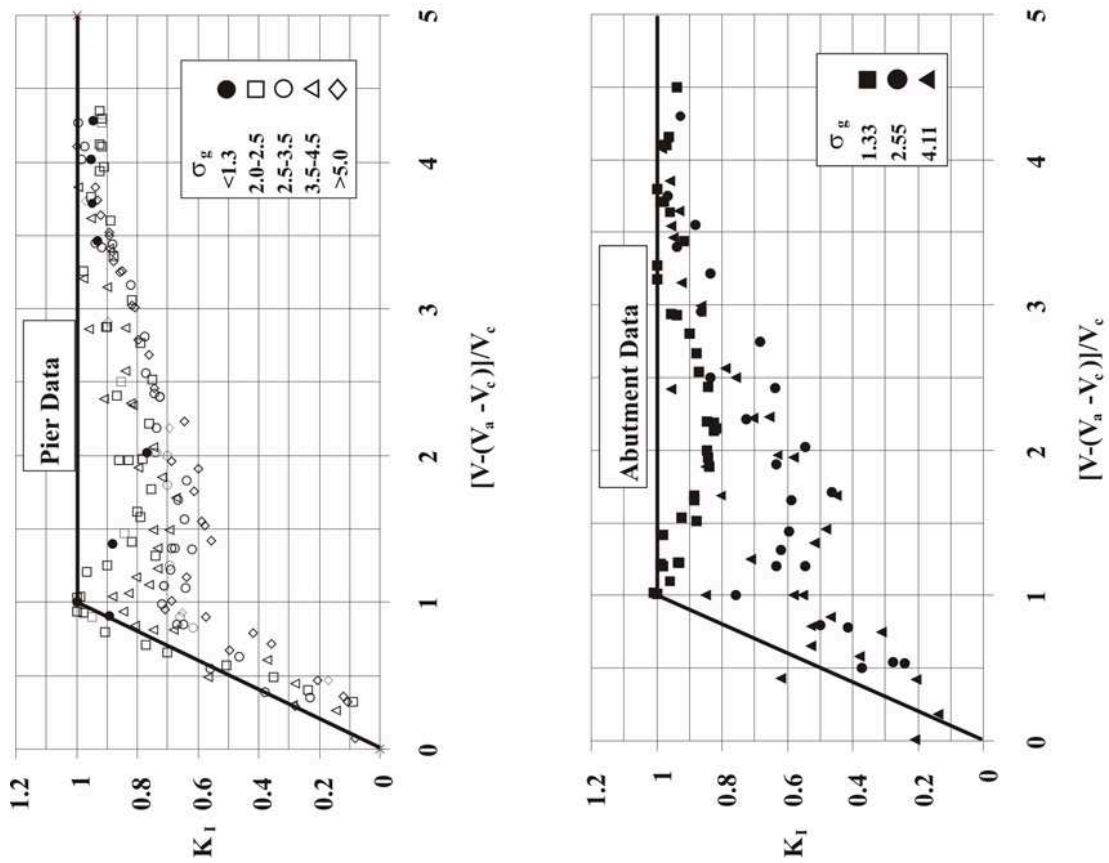


Figure 6 Influence of flow intensity on local scour depth in nonuniform sediment

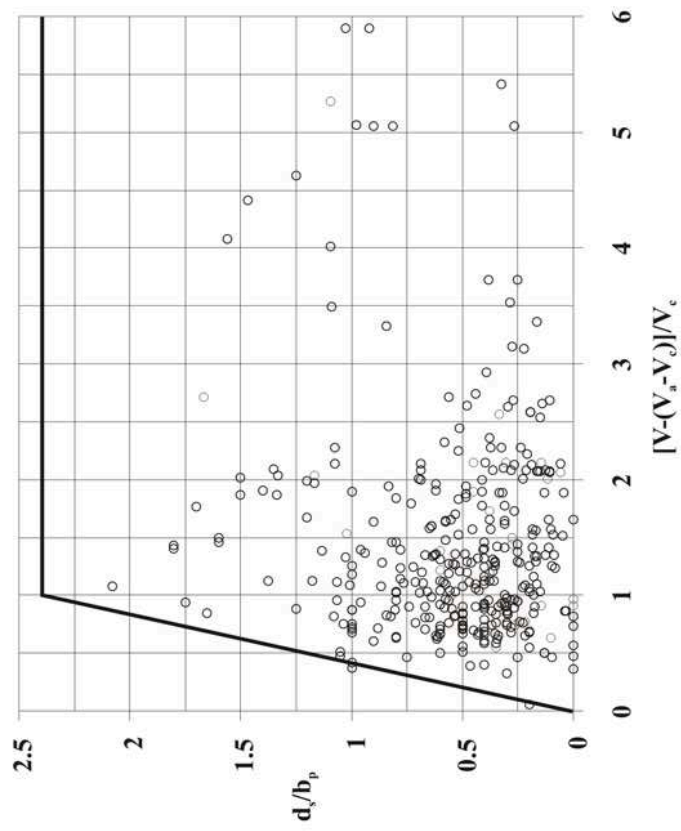


Figure 7 Comparison of field data with flow intensity curves

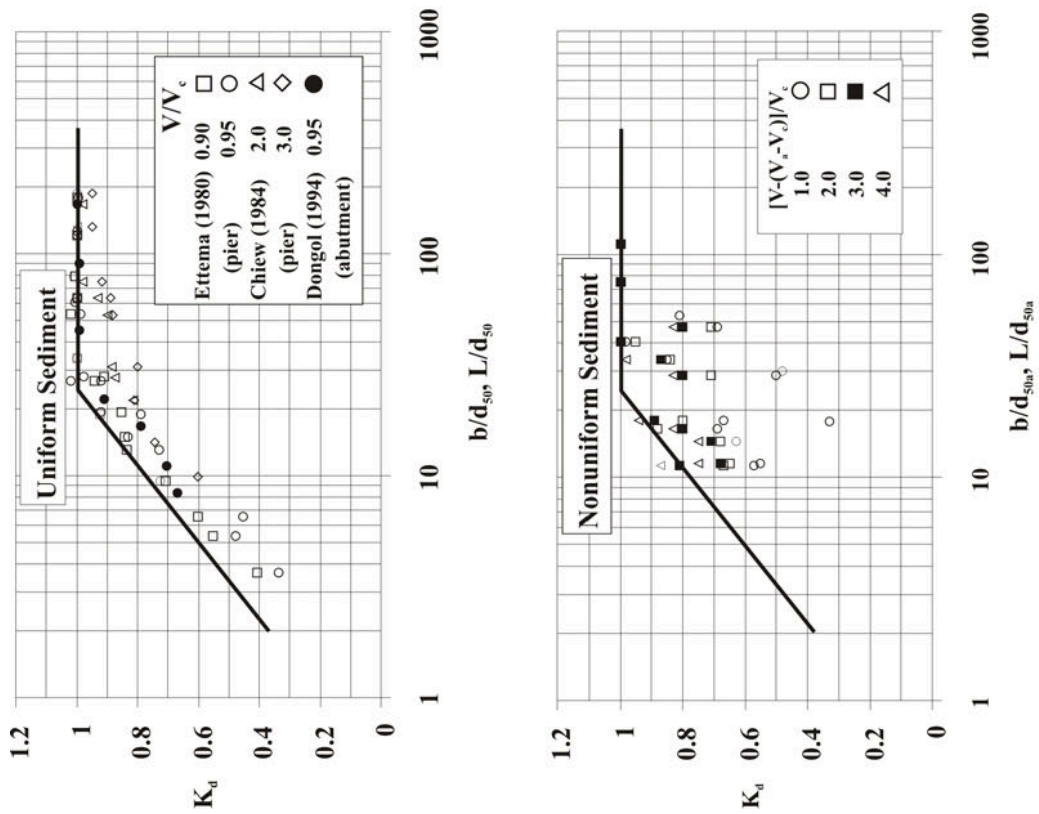


Figure 8 Influence of sediment coarseness on local scour depth

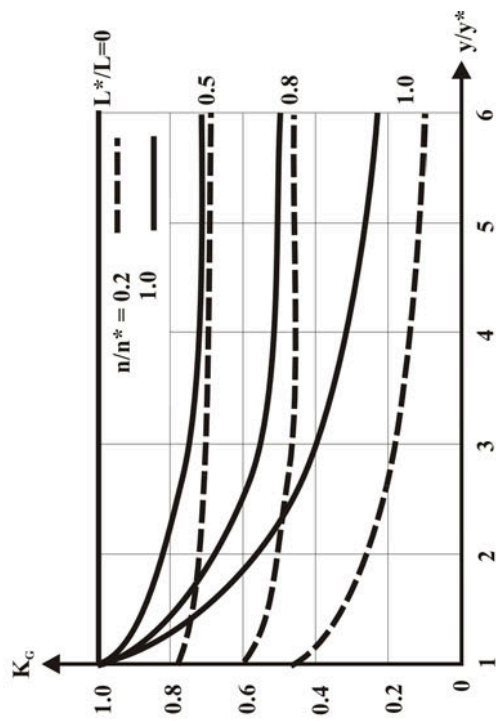
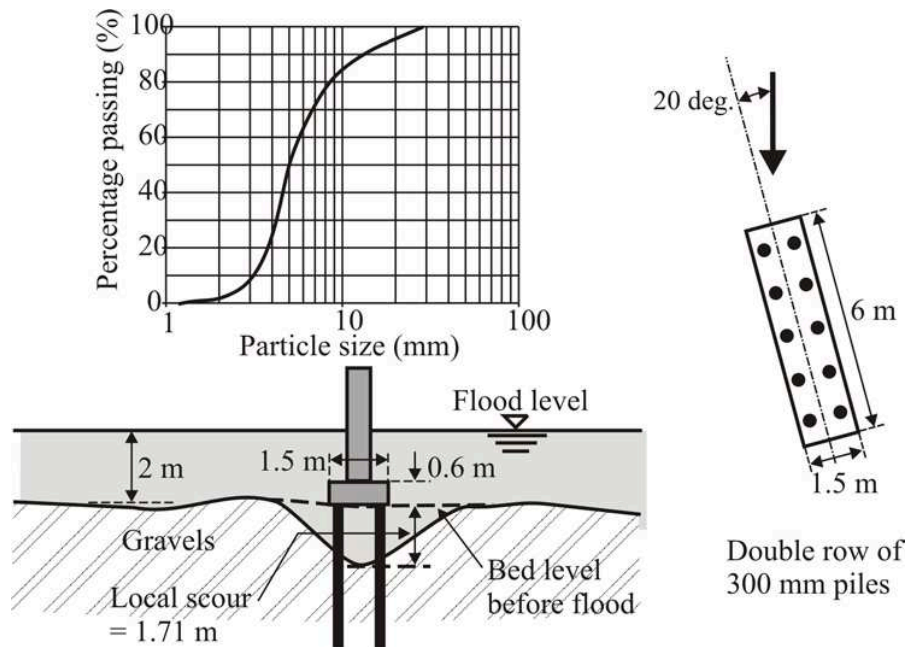
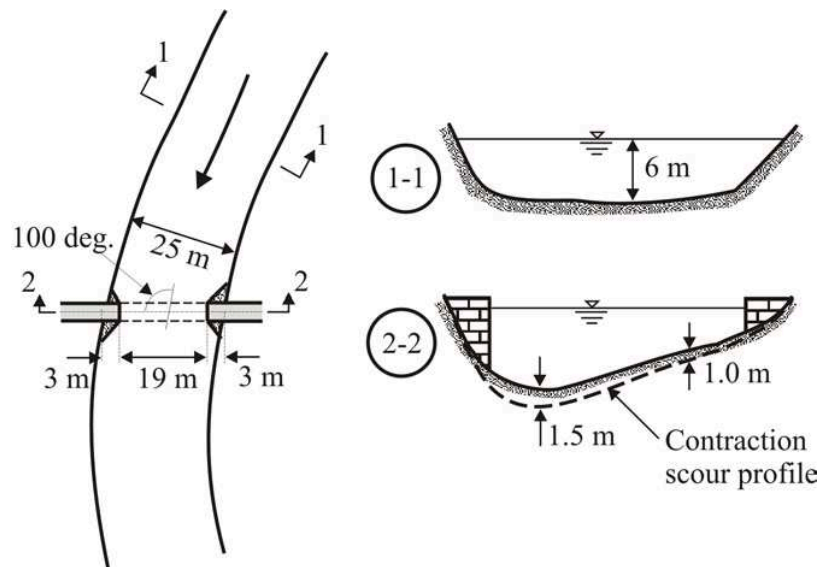


Figure 9 Influence of channel geometry on local scour depth at bridge abutments



**Figure 10** Diagram for pier scour example



**Figure 11** Diagram for abutment scour example